

Quantum dynamics of evaporatively cooled Bose-Einstein condensates

P. D. Drummond and J. F. Corney

Department of Physics, The University of Queensland, St. Lucia, Queensland, Australia 4072

(Received 21 May 1999)

We report on dynamical simulations of Bose-Einstein condensation via evaporative cooling in an atomic trap. The results show evidence for spontaneous vortex formation and quantum dynamics in small traps. [S1050-2947(99)50110-8]

PACS number(s): 03.75.Fi, 05.30.Jp, 32.80.Pj, 42.50.Lc

Evaporative cooling has been successfully used to produce Bose-Einstein condensates (BEC's) inside magneto-optic traps with neutral atoms [1]. A number of questions arise as to the quantum state that is achieved, since this involves both the dynamics of the cooling process and the applicability of the ergodic hypothesis. Atom-atom interactions have a strong influence on the cooling process and the final state in these experiments. Quantum fluctuations are important in determining atom laser coherence properties [2], especially since the experimental systems do not have as large a particle number as traditional condensed matter experiments. However, there is no guarantee that a canonical ensemble will result from evaporative cooling, as the observations are made in a transient, nonequilibrium phase. Thus, conventional canonical methods may not be applicable to these experiments.

In this paper, we report the use of phase-space methods for direct quantum-dynamical calculations of the cooling and formation of Bose-Einstein condensates on a three-dimensional lattice. The results are restricted as yet to three condensates, due to the large numbers of modes involved. The computational results are very similar to those observed experimentally. In particular, we find quantum evaporative cooling, followed by a clear transition to a condensate. This is strongly influenced by nonclassical features of the quantum dynamics. The calculations indicate additional structure, which we interpret as spontaneous formation of vortices—a process of much wider interest in other fields of physics [3]. These appear to originate in the residual orbital angular momentum of the trapped atoms, which was neglected in previous studies, and would provide a significant test of the present theory.

Earlier calculations of cooling dynamics have usually treated the cooling process either classically [4,5], or have used various additional assumptions about the quantum states involved. This leads to the question of how to handle the transition to the final quantum dominated condensate, which is often assumed to be a canonical ensemble at a temperature estimated from the classical theory. The final ensemble behavior is then usually calculated from the mean-field Gross-Pitaevskii equations [6], although some attempts have been made to go beyond this [7], including treatment of the kinetics of condensation [8,9] based on a master equation. However, small atom traps are neither in the thermodynamic limit, nor necessarily in a steady state. A first-principles theory is really needed, to provide a benchmark

for comparisons of these previous approximations, like the quantum Monte Carlo theories (QMTs) [10] in equilibrium systems.

In our calculations, we include 3×10^4 relevant modes (which is a very conservative estimate), with up to 1.0×10^4 atoms present. The quantum-state vector therefore has over $10^{10\,000}$ components. One possible approach in principle is to use quantum-number-state calculations in the time domain. Any direct calculation that includes all the relevant modes of the trapped atoms—up to the energy scales required for evaporating atoms to escape—is easily seen to be an enormous computational problem.

A more practical technique is to utilize phase-space methods that have already proved successful in laser theory. These techniques can handle large numbers of particles, but can also systematically treat departures from classical behavior, including boson interactions. Generalized phase-space representations were used to correctly predict quadrature squeezed quantum soliton dynamics in optical fibers [11], which are described by quantum equations nearly identical to those used in atom-atom interaction studies. The coherent-state (positive- P) phase-space equations are exactly equivalent to the relevant quantum equations, provided phase-space boundary terms [11] vanish. They have the advantage that they are computationally tractable for the large Hilbert spaces typical of BEC experiments. Techniques of this sort can provide a first step towards extending QMT methods [10] into the time domain.

The model that we use includes the usual nonrelativistic Hamiltonian for neutral atoms in a trap $V(\mathbf{x})$, interacting via a potential $U(\mathbf{x})$, together with absorbing reservoirs $\hat{R}(\mathbf{x})$, in $d=2$ or $d=3$ dimensions:

$$\begin{aligned} \hat{H} = & \int d^d \mathbf{x} \left[\frac{\hbar^2}{2m} \nabla \hat{\Psi}^\dagger(\mathbf{x}) \nabla \hat{\Psi}(\mathbf{x}) + V(\mathbf{x}) \hat{\Psi}^\dagger(\mathbf{x}) \hat{\Psi}(\mathbf{x}) \right. \\ & + \hat{\Psi}^\dagger(\mathbf{x}) \hat{R}(\mathbf{x}) + \hat{\Psi}(\mathbf{x}) \hat{R}^\dagger(\mathbf{x}) \\ & \left. + \frac{1}{2} \int d^d \mathbf{y} U(\mathbf{x}-\mathbf{y}) \hat{\Psi}^\dagger(\mathbf{x}) \hat{\Psi}^\dagger(\mathbf{y}) \hat{\Psi}(\mathbf{y}) \hat{\Psi}(\mathbf{x}) \right]. \quad (1) \end{aligned}$$

Here $\hat{R}(\mathbf{x})$ represents a localized absorber that removes the neutral atoms; for example, via collisions with foreign atoms, or at the location of the ‘‘rf-scalpel’’ resonance, which is used to cause evaporative cooling [1]. We expand $\hat{\Psi}$ using free-field modes with a momentum cutoff k_{max} .

Provided that $k_{max} \ll a_0^{-1}$, where a_0 is the S -wave scattering length, $U(\mathbf{x}-\mathbf{y})$ can be replaced by the renormalized pseudopotential $u\delta^d(\mathbf{x}-\mathbf{y})$, where $u=4\pi a_0\hbar^2/m$ in three dimensions. In two dimensions, u is defined similarly, but with a factor ξ_0 in the denominator, which corresponds to the effective spatial extent of the condensate in the third direction. This factor is of the order of the lattice spacing in the simulation, and is chosen to be equal to x_0 , the scaling length.

The resulting quantum time evolution for the density matrix $\hat{\rho}$ can be solved by expanding into a coherent-state basis, and then (provided phase-space boundary terms vanish) transforming to an equivalent set of equations in the positive- P representation. The phase-space equations in the BEC case can be expressed as two coupled complex partial stochastic differential equations of the form

$$i\hbar \frac{\partial \psi_j}{\partial t} = \left[\frac{-\hbar^2}{2m} \nabla^2 + u \psi_j \psi_{3-j}^* + V(\mathbf{x}) - \frac{i\hbar}{2} \Gamma(\mathbf{x}) + \sqrt{i\hbar} u \xi_j(t, \mathbf{x}) \right] \psi_j, \quad (2)$$

where $j=1,2$ and where the stochastic fields ψ_j are the coherent-state amplitudes of a nondiagonal coherent-state projector, $|\psi_1\rangle\langle\psi_2|/\langle\psi_2|\psi_1\rangle$. These equations can be readily simulated numerically [12] in one, two, or three transverse dimensions, with either attractive or repulsive potentials. The form of the potentials was chosen to be

$$V(\mathbf{x}, t) = (1 - \alpha t) V_{max} \sum_{j=1}^d [\sin(\pi x_j/L_j)]^2, \quad (3)$$

where α is typically the inverse of the total simulation time. The potential height was swept downwards linearly in time, thus successively removing cooler and cooler subpopulations of atoms. The absorption rate $\Gamma(\mathbf{x})$ was chosen as

$$\Gamma(\mathbf{x}) = \Gamma_{max} \sum_{j=1}^d [\sin(\pi x_j/L_j)]^{50}. \quad (4)$$

Here L_j is the trap width in the j th direction, such that $-L_j/2 \leq x_j \leq L_j/2$. The sinusoidal shape of the potential and absorption was chosen so that the trap would be harmonic near the center of the trap, and smoothly approach a maximum near the edge. Thus hot atoms are absorbed when they reach regions of large $\Gamma(\mathbf{x})$, located near the trap edges.

A useful feature of Eq. (2) is that, in the deterministic limit, this corresponds precisely to the well-known Gross-Pitaevskii equations, with the addition of a coefficient $\Gamma(\mathbf{x})$ for the absorption of atoms by the reservoirs. Quantum effects come from the terms ξ_j , which are real Gaussian stochastic fields, with correlations:

$$\langle \xi_1(s, \mathbf{x}) \xi_2(t, \mathbf{y}) \rangle = \delta_{ij} \delta(s-t) \delta^d(\mathbf{x}-\mathbf{y}). \quad (5)$$

The quantum correlations that can be calculated include $n(\mathbf{k}) = \langle \psi_1(\mathbf{k}) \psi_2^*(\mathbf{k}) \rangle$, which gives the observed momentum distribution.

The results of the simulations depend critically on the exact parameters chosen, just as one would expect from the

known sensitivity of the experiments to the precise experimental conditions. In practical computations, it is necessary to consider rather small traps. This is because the numerical lattice spacing used to sample the stochastic fields in x space must be of order $\Delta x = 1/k_{max}$, where k_{max} is the largest ordinary momentum considered in the problem. However, the value of the corresponding kinetic energy, $E_K = (\hbar k_{max})^2/2m$, must be large enough to allow energetic atoms to escape over the potential barrier of the trap; otherwise, no cooling can take place. This sets an upper bound on the lattice spacing, and hence on the maximum trap size, which depends on the number of lattice points that can be computed.

The available lattice sizes used here were 32^d points, depending on the dimensionality d . With this limit, and parameter values similar to those used in the experiments, the available trap sizes that can be treated are of the order of micron dimensions. These are smaller than those used currently, although traps of this type are quite feasible. The other possibility within the constraints is to use a trap that is of larger dimensions but lower in potential height. For this type of trap, which was simulated here, the width was $L_j = 10 \mu\text{m}$, with a potential height of $V_{max}/k_B = 1.9 \times 10^{-7}$ K and an initial temperature of $T_0 = 2.4 \times 10^{-7}$ K.

For physical reasons, a further limitation is that the initial density must be such that $\langle n(k) \rangle \leq 1$; otherwise, the starting point would already have a Bose-Einstein condensation. This places a limit on the number of atoms that can be simulated, if we assume an initially noncondensed grand-canonical ensemble of (approximately) noninteracting atoms. There were initially around 500 atoms in the two-dimensional simulations reported here and 10 000 in the three-dimensional case. These corresponded to atomic densities of $n_0 = 5.0 \times 10^{12}/\text{m}^2$ and $n_0 = 1.0 \times 10^{19}/\text{m}^3$, respectively.

For the small trap parameters used in the simulations, the effect of the stochastic terms on the dynamics is very large. In fact, the quantum fluctuations that these stochastic terms introduce are much larger than the initial thermal fluctuations, such that the initial features of the distribution do not persist. This means that the choice of the initial state of the system is not critical, and also that in order to determine properties of the final quantum ground state of the system, the stochastic terms are vital. For comparison, we investigated the effect of removing the quantum noise terms, so that the simulations were simply of the Gross-Pitaevskii equation, with initial conditions corresponding to a thermal state. For our parameters, these situations did not show strong Bose condensation effects, in contrast to the fully quantum-mechanical simulations. This demonstrates the highly nonclassical nature of the early stages of Bose condensation, in which spontaneous transitions to the lowest-energy states clearly play an important role.

For the simulations shown in the figures, $a_0 = 0.6$ nm and the mass, corresponding to rubidium, is $m = 1.5 \times 10^{-25}$ kg. These parameters correspond to relatively weakly interacting atoms, in order to reduce the sampling error—which increased rapidly with longer times and larger coupling constants. No large phase-space excursions were observed with these parameters. All results are plotted in normalized units, with space scaled by $x_0 = 0.76 \mu\text{m}$ and time scaled by $t_0 = 0.79$ ms. The time step was typically $t_0/2500$, with all

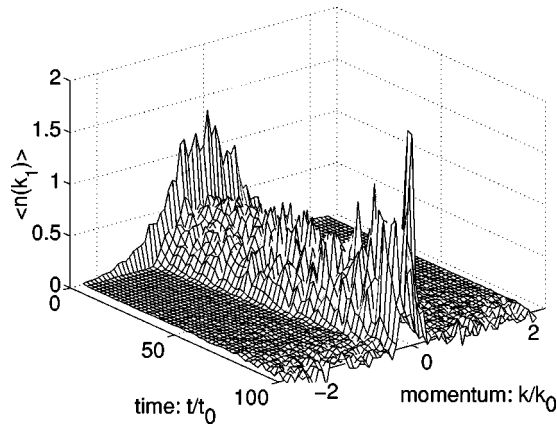


FIG. 1. Simulation of a two-dimensional Bose condensate, showing the ensemble average (55 paths) atom density $\langle n(k) \rangle$ along one dimension in Fourier space versus time. Time has been normalized by $t_0 = 0.79$ ms and momentum by $k_0 = 1.32 \times 10^6 m^{-1}$.

calculations being repeated at half the time step (and noise sampled from the same process with twice the resolution [12]), to check numerical convergence. The boundary absorption term was set to $\Gamma_{max} \approx 10^3/s$.

In momentum space, the final atom density for individual trajectories in both two and three dimensions is quite narrow and tall, with a width corresponding to a temperature well below the critical temperature for BEC. The peak final momentum state population is much greater than 1 (and greater than the initial conditions). This is more pronounced in the three-dimensional case than in two dimensions, showing that the evaporative cooling process is more efficient with the extra degree of freedom and the greater number of atoms that are present.

As is usual in quantum mechanics, only the ensemble averages of the simulations have an operational meaning. Thus, while individual stochastic realizations have a definite coherent phase, these phases are different for distinct stochastic realizations—the ensemble average has no absolute phase information. The average evolution of a two-dimensional condensate is shown in Fig. 1; in this case, the condensate is only weakly occupied.

Since the condensate does not have to form in the ground state, the Bose-condensed peaks that occur at different momentum values in single runs are averaged out in the overall ensemble. A more useful indication of condensation is given by the following measure of phase-space confinement:

$$Q = \frac{\int d^3k \langle \psi_1(\mathbf{k}) \psi_1(\mathbf{k}) \psi_2^*(\mathbf{k}) \psi_2^*(\mathbf{k}) \rangle}{\left(\int d^3k \langle \psi_1(\mathbf{k}) \psi_2^*(\mathbf{k}) \rangle \right)^2 x_0^3}. \quad (6)$$

This higher-order correlation function is the quantum analogue of the participation ratio defined by Hall [13]. Figure 2 shows the evolution of Q calculated from 15 runs of the three-dimensional simulation. The sharp rise near $t = 100$ is a strong indication of condensation occurring at this point.

For the finite-size condensates in atom traps, just as the final ground state is not expected to be precisely the zero momentum eigenstate, so too such condensates are not con-

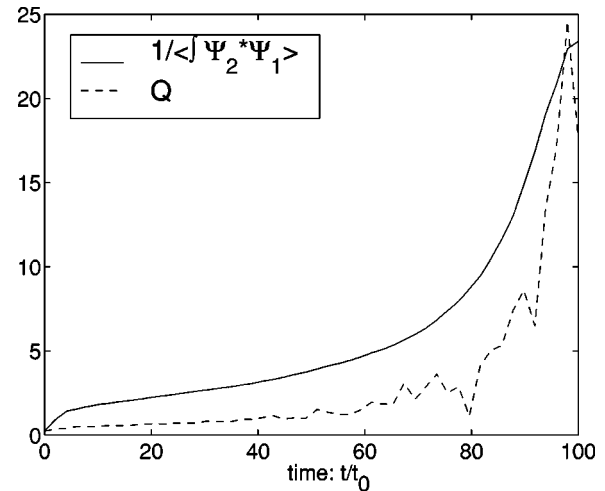


FIG. 2. Simulation of a three-dimensional Bose condensate, showing the ensemble average evolution (15 paths) of the confinement parameter Q . The time axis has been normalized by $t_0 = 0.79$ ms.

strained to fall into the $J=0$ angular-momentum eigenstate. Both the initial and the escaping atoms have an arbitrary angular momentum. We can estimate that the variance in angular momentum will scale approximately as $\langle \hat{J}^2 \rangle \propto N$, from central limit theorem arguments. Thus, we can expect that each trapped condensate should have angular momentum, unless constrained by the trap geometry. The angular momentum can be carried either by quasiparticles or vortices, although a volume-filling j th-order vortex has $J = Nj$ and therefore cannot form spontaneously in the thermodynamic limit of large N . For small condensates, a $j = \pm 1$ vortex may be quite likely. Several authors [14] have considered how such vortex states may form through stirring or rotating a condensate, and the stability of vortices has been explored [15]. Here we consider the possibility of vortices forming spontaneously in the condensate through the process of evaporative cooling, without external intervention.

The presence of vortex states can be detected quantitatively by transforming the spatial lattice into a lattice that uses the angular-momentum eigenstates as a basis set. The

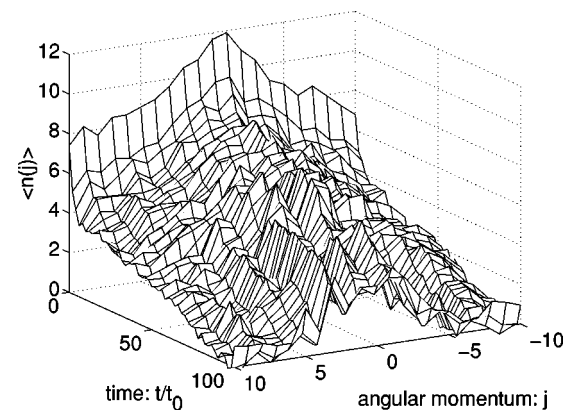


FIG. 3. Ensemble average of the angular-momentum distribution $\langle n(j) \rangle$, during the condensation of a two-dimensional Bose condensate (40 paths). The time axis has been normalized by $t_0 = 0.79$ ms.

two-dimensional results, which are presented here, are obtained by integrating the spatial profile over orthogonal modes with corresponding field operators $\hat{\Psi}_{jn}$. The angular-momentum distribution is then given by a summation over the radial modes:

$$n(j) = \sum_n \langle \hat{\Psi}_{jn} \hat{\Psi}_{jn}^* \rangle. \quad (7)$$

The angular-momentum distribution for individual trajectories shows large occupation in particular angular modes, different for each run. This indicates that vortices with different momenta appear each time. For example, in one run, a vortex with $j = -1$ appears at about one-quarter of the way through the simulation, and persists until the end. The maximum occupation of the vortex is around $n(j) = 20$, owing to relatively small initial atom numbers in this two-dimensional

trap simulation. Shown in Fig. 3 is the ensemble average of the angular-momentum distribution, which reveals quite a broad range of final angular momentum. This is consistent with the existence of vortices.

In summary, we have demonstrated a three-dimensional real-time quantum-dynamical simulation of Bose condensation with mesoscopic numbers of interacting atoms on a large lattice. Sampling errors and lattice size restrictions impose strong limitations on these initial simulations. The results, as well as showing evidence for highly nonclassical behavior in a first-principles simulation of BEC formation, indicate the possibility of spontaneous vortex formation in small evaporatively cooled condensates.

This research was supported in part by the Australian Research Council, and by the National Science Foundation under Grant No. PHY94-07194.

-
- [1] M. H. Anderson, J. R. Ensher, C. E. Wieman, and E. A. Cornell, *Science* **269**, 198 (1995); C. C. Bradley, C. A. Sackett, J. J. Tollett, and R. G. Hulet, *Phys. Rev. Lett.* **75**, 1687 (1995); K. B. Davis, M. O. Mewes, M. R. Andrews, N. J. van Druten, D. S. Durfee, D. M. Kurn, and W. Ketterle, *ibid.* **75**, 3969 (1995).
- [2] M.-O. Mewes, M. R. Andrews, D. M. Kurn, D. S. Durfee, C. G. Townsend, and W. Ketterle, *Phys. Rev. Lett.* **78**, 582 (1997).
- [3] W. H. Zurek, *Nature (London)* **317**, 505 (1985).
- [4] K. Burnett, *Contemp. Phys.* **37**, 1 (1996); K. B. Davis, M. O. Mewes, and W. Ketterle, *Appl. Phys. B: Photophys. Laser Chem.* **60**, 155 (1995); W. Ketterle and N. J. Van Druten, *Adv. At., Mol., Opt. Phys.* **37**, 181 (1996).
- [5] K. Berg-Sorensen, *Phys. Rev. A* **55**, 1281 (1997); H. Wu, E. Armondo, and C. J. Foot, *ibid.* **56**, 560 (1997).
- [6] M. Bijlsma and H. T. C. Stoof, *Phys. Rev. A* **55**, 498 (1997); K. Damle, S. N. Majumdar, and S. Sachdev, *ibid.* **54**, 5037 (1996); V. M. Perez-Garcia, H. Michinel, J. I. Cirac, M. Lewenstein, and P. Zoller, *ibid.* **56**, 1424 (1997); Yu. Kagan and B. V. Svistunov, *Phys. Rev. Lett.* **79**, 3331 (1997).
- [7] K. Ziegler and A. Shukla, *Phys. Rev. A* **56**, 1438 (1997); E. Braaten and A. Nieto, *Phys. Rev. B* **56**, 14 745 (1997).
- [8] C. W. Gardiner, P. Zoller, R. J. Ballagh, and M. J. Davis, *Phys. Rev. Lett.* **79**, 1793 (1997); D. Jaksch, C. W. Gardiner, K. M. Gheri, and P. Zoller, *Phys. Rev. A* **58**, 1450 (1998); C. W. Gardiner and P. Zoller, *ibid.* **58**, 536 (1998); D. Jaksch, C. W. Gardiner, and P. Zoller, *ibid.* **56**, 575 (1997); C. W. Gardiner and P. Zoller, *ibid.* **55**, 2902 (1997).
- [9] M. Holland, J. Williams, and J. Cooper, *Phys. Rev. A* **55**, 3670 (1997); L. I. Plimak and D. F. Walls, *ibid.* **54**, 652 (1996).
- [10] D. M. Ceperley, *Rev. Mod. Phys.* **67**, 279 (1995).
- [11] S. J. Carter, P. D. Drummond, M. D. Reid, and R. M. Shelby, *Phys. Rev. Lett.* **58**, 1841 (1987); P. D. Drummond, R. M. Shelby, S. R. Friberg, and Y. Yamamoto, *Nature (London)* **365**, 307 (1992); A. Gilchrist, C. W. Gardiner, and P. D. Drummond, *Phys. Rev. A* **55**, 3014 (1997); M. Steel, M. Olsen, L. Plimak, P. D. Drummond, S. Tan, M. J. Collet, D. F. Walls, and R. Graham, *ibid.* **58**, 4824 (1998).
- [12] M. J. Werner and P. D. Drummond, *J. Comput. Phys.* **132**, 312 (1997).
- [13] M. J. W. Hall, *Phys. Rev. A* **59**, 2602 (1999).
- [14] K.-P. Marzlin, W. Zhang, and E. M. Wright, *Phys. Rev. Lett.* **79**, 4728 (1997); R. J. Dodd, K. Burnett, M. Edwards, and C. W. Clark, *Phys. Rev. A* **56**, 587 (1997); M. Edwards, R. J. Dodd, C. W. Clark, P. A. Ruprecht, and K. Burnett, *ibid.* **53**, R1950 (1996); E. Lundh, C. J. Pethick, and H. Smith, *ibid.* **55**, 2126 (1997); S. Sinha, *ibid.* **55**, 4325 (1997).
- [15] D. S. Rokhsar, *Phys. Rev. Lett.* **79**, 2164 (1997).